Received October 22, 2020, accepted November 8, 2020, date of publication November 11, 2020,
date of current version November 30, 2020.

Digital Object Identifier 10.1109/ACCESS.2020.3037510

Field Current Waveform-Based Method for Estimation of Synchronous Generator Parameters Using Adaptive Black Widow Optimization Algorithm

MIHAILO MICEV[1], (Student Member, IEEE), MARTIN ĆALASAN[1], (Member, IEEE), DRAGAN S. PETROVIĆ[2], ZIAD M. ALI[3,4], NGUYEN VU QUYNH[5], AND SHADY H. E. ABDEL ALEEM[6], (Member, IEEE)

[1]Faculty of Electrical Engineering, University of Montenegro, 81000 Podgorica, Montenegro
[2]School of Electrical Engineering, University of Belgrade, 11000 Belgrade, Serbia
[3]Electrical Engineering Department, College of Engineering at Wadi Addawaser, Prince Sattam Bin Abdulaziz University, Wadi Addawasir 11991, Saudi Arabia
[4]Electrical Engineering Department, Aswan Faculty of Engineering, Aswan University, Aswan 81542, Egypt
[5]Electrical and Electronics Department, Lac Hong University, Bien Hoa 810000, Vietnam
[6]Mathematical, Physical and Engineering Sciences, 15th of May Higher Institute of Engineering, Cairo 11721, Egypt

Corresponding authors: Shady H. E. Abdel Aleem (engyshady@ieee.org) and Nguyen Vu Quynh (vuquynh@lhu.edu.vn)

This work was supported by Lac Hong University, Vietnam, under Grant LHU-RF-TE-19-04-03.

ABSTRACT This article presents a novel method for identification of synchronous generator parameters that is based on sudden short-circuit test data and a novel metaheuristic algorithm, called the adaptive black widow optimization algorithm. Unlike traditional methods defined by IEEE and International Electrotechnical Commission (IEC) standards, which rely on the armature current oscillogram, the method proposed in this article uses the field current waveform during the short-circuit test. Moreover, the standard graphical method for extraction of the generator parameters is replaced by an effective metaheuristic algorithm. The proposed algorithm tends to minimize the normalized sum of squared errors (NSSE) between simulation and experimental results. The applicability and accuracy of the proposed optimization technique are verified using experimentally obtained results from a 100-MVA synchronous generator at the Bajina Basta hydropower plant.

INDEX TERMS Black widow optimization algorithm, field current waveform, parameter estimation, synchronous generator.

NOMENCLATURE

d, q	d-axis and q-axis quantities
d	Dimension of the optimization problem
f, a	Field and armature quantities
kd, kq	d-axis damper winding and q-axis damper winding quantities
i	Current
i_{f0}	Field current before short-circuit
$I_{f,exp}$	Experimental field current
$I_{f,sim}$	Simulated field current
L	Leakage inductance
L_{md}	Mutual inductance between windings on d-axis
L_{mq}	Mutual inductance between windings on q-axis
N	Size of the population
R	Resistance
t	Time
T_a	Armature winding time constant
T'_d	Direct-axis transient short-circuit time constant
T''_d	Direct-axis subtransient short-circuit time constant
T_{kd}	Direct-axis damper leakage time constant
u	Voltage
X	Reactance
$\boldsymbol{x}_1$, $\boldsymbol{x}_2$	Randomly chosen parents from the population
X_d	Direct-axis synchronous reactance
X'_d	Direct-axis transient reactance
$\boldsymbol{y}_1$, $\boldsymbol{y}_2$	Offsprings created of the population

The associate editor coordinating the review of this manuscript and approving it for publication was Wei Xu.

ψ Flux linkage
ω Angular speed
ω_0 Synchronous speed
θ Vector of estimated parameters

I. INTRODUCTION

Among the many different types of electric generators found in power systems, including synchronous generators, double-fed induction generators, permanent magnet generators, switched reluctance generators, and so on, the first type is the most widely used in electric power plants. Modeling and steady-state and transient analysis of synchronous generators are a crucial part of power system analysis [1], [2].

Estimation of synchronous generator parameters has been a very important topic of research in recent years, as shown by the development of standardized test procedures by IEC and IEEE [3], [4]. Most of the procedures in the mentioned standards are based on graphical extraction of the parameters from armature current oscillograms during three-phase short-circuit tests. The graphical methods are actually geometrical, which means they are subject to human error. Moreover, the armature current is measured using current transformers, which are subject to saturation. Despite the existence of standard test procedures, many studies have been performed to demonstrate different non-standard methods for the determination of synchronous generator parameters. Among the most frequently used are load rejection [5]–[9] and field flashing [9] tests. Load rejection test consists of two steps, in which d-axis parameters are determined in the first step, while q-axis parameters are determined in the second step. Precisely, to determine d-axis parameters, the generator's excitation system is set to manual mode, and the generator is operating with 0 active power and 0.1 pu absorption of reactive power. After achieving such an operating point, the breaker can be opened to reject the load. It is then necessary to measure the generator's voltage to determine the parameters [5]–[9]. Similarly, in the q-axis test, the generator's power factor angle needs to be equal to the rotor angle, which is approximately achieved when the generator operates with 0.1 pu active power and a few percent of nominal reactive power (absorption, as in d-axis test). When the mentioned condition is met, the second step of the test can be conducted by opening the breaker. Field flashing test, used in [9], consists of a slight increase of the field voltage to supply initial excitation of the generator and incrementally increase the terminal voltage to 1 pu. This test is conducted when the armature circuit is opened. The methods of parameter extraction are different: Levenberg-Marquardt is used in [5], asymptotic weighted least squares is applied in [6], [7], the standard graphical method is used in [8], and the interior point method is demonstrated in [9]. It is also important to mention that the authors of [8] proposed an improved load rejection method that takes into account the effects of saturation, while variations of the field voltage are considered in [9]. Furthermore, many authors have developed parameter estimation methods based on phasor measurement unit (PMU) data [10]–[16], in which PMUs provide the data about voltage magnitude and phase, rotor position, angular speed, stator current, and electrical power at the generator bus. These data are essential for applying the extraction methods presented in [10]–[16]. Extraction of the parameters can be carried out using a dynamic state estimator based on Kalman filters [10]–[12], modified least-squares (LS) algorithm [13], genetic algorithms (GAs) [14], adaptive importance sampling combined with Bayesian inference [15], and the primal-dual interior points (PDIP) method [16]. Test methods that rely on measuring field and armature voltage and current are proposed in a significant number of recent studies [17]–[26]. Authors have demonstrated the use of a large variety of methods for the determination of the parameters: nonlinear LS is used in [17], [18], while the LS algorithm along with observers for estimation of damper current is applied in [19]–[21], nonlinear mapping is demonstrated in [22], and the use of Hartley series is proposed in [23]. An improved dynamic state estimator called the Unscented Kalman filter (UKF) is used in [24], a univariate search method is applied in [25], and a maximum likelihood algorithm is demonstrated in [26]. A large number of the test procedures are conducted while the generator is at standstill; one of the most popular is the chirp test, which is combined with the hybrid GA–quasi-Newton method in order to determine synchronous generator parameters [27]. Chirp signal stands for the linear swept-frequency sinusoidal signal. The chirp test is carried out by applying a chirp signal to the stator windings while the field winding is short-circuited and the generator is at a standstill. By measuring stator voltage and currents and the field current, parameters of the generator can be extracted. In studies presented by Arjona, the GA algorithm combined with the Gauss-Newton method is used to extract the parameters when two standstill tests are applied: sine cardinal perturbation in [28] and a step voltage test in [29]. These test methods are very similar to the previously described chirp test. In [28], a sine signal is applied to the stator winding instead of a chirp signal. Also, in [29], a step voltage signal is applied between two of the stator terminals. In both cases, the field winding is short-circuited, and the rotor is stationary. Application of the pseudo-random binary sequence (PRBS) excitation voltage at the field winding is demonstrated in [30]–[32], while another standstill test, called the dc-flux decay test, is applied in [32], [33]. The field winding must be short-circuited, and the generator must be at a standstill during this test (like the previously described standstill tests). Initially, a constant direct current is applied at the stator windings, setting up the machine's magnetic flux. After the excitation current reaches a steady-state, the direct current is turned off, and the stator windings are short-circuited. The stator current waveform during the short-circuit is used to extract the generator parameters. The optimization or extraction methods are different and include the H-infinity [30], hybrid particle swarm optimization-quantum operation (PSO-QO) [31], Levenberg-Marquardt [32], and maximum

likelihood algorithms [33]. Short-circuit tests are part of the standardized procedures described in [3], [4] but are also used in combination with different optimization or determination methods: the Knitro optimization solver [34], graphical methods [35], curve-fitting techniques [36], the LS algorithm [37], and the nonlinear Lasso method [38]. Except for short-circuit faults, parameters can be determined when remote line-to-line faults are considered with the use of the PSO algorithm, as described in [39]. The current injection test method, along with the GA algorithm, is proposed in [11], while a method combining use of online measured data from the terminals of the generator in the case of the disturbance and an artificial neural network (ANN) observer is presented in [40]. An approach based on measuring field current during a short circuit is presented in [41]. Namely, in [41], a numerical procedure for synchronous machine parameters determination is based on minimization of the sum of squared errors (SE) between the periodic and aperiodic components of the experimentally obtained field current waveform, and the analytical waveforms. In [42], UKF is applied to extract synchronous generator parameters under unbalanced operating conditions, while in [43], the estimation of dynamic states (rotor angle and speed) under unknown measurement noise using robust cubature Kalman filter (CKF) is demonstrated.

In this regard, the large list of papers dealing with synchronous machine parameters estimation demonstrates the importance of the topic. On the other hand, the use of different methods in the previously mentioned papers reveals that there is room for improvement and that we still have not found the best one.

In this article, the field current waveform during a sudden three-phase short circuit of an unloaded generator will be used to obtain the transient parameters. In this way, all time constants and short-circuit time constants except the subtransient reactance can be estimated. In the available literature, short-circuit tests are conducted with the purpose of measuring the armature current and using its oscillograms to calculate the machine parameters. This article proposes the use of the field current, whose analytical expression does not contain the double-frequency component, which can significantly increase the accuracy of the results. Moreover, the field current is measured using shunt resistors, which do not have saturation problems, unlike the current transformers used for measuring armature current, as mentioned before. Furthermore, a novel metaheuristic algorithm is proposed as a tool for extracting the synchronous generator parameters from the field current waveform (based on measuring field current during a short circuit). The parameters of the generator are obtained by applying a numeric algorithm with predefined error tolerance. It is essential to mention that other computational intelligence algorithms can solve the optimization problem considered using the methodology proposed in this work. Some of the most representative computational intelligence algorithms are monarch butterfly optimization (MBO) [44], earthworm optimization algorithm (EWA) [45], elephant herding optimization (EHA) [46], moth search algorithm (MSA) [47], and others.

The contribution of this article is twofold. First, a novel method for determining synchronous generator parameters based on measuring the field current during the short circuit is presented. Compared to the existing approaches, this method is characterized by its simplicity and very high accuracy. Second, a novel metaheuristic algorithm, called adaptive black widow optimizer (ABWO), is proposed. The performance of ABWO is compared with various computational intelligence algorithms, and it proved its superiority in terms of convergence speed and the accuracy of the obtained results. The proposed algorithm's performance was tested with some high-dimensional and multimodal benchmark functions. These tests proved the proposed method's scalability and applicability to solve high-dimensional optimization problems. Also, good results obtained with multimodal test functions show that the ABWO algorithm can efficiently handle premature convergence.

This article is organized as follows. A short overview of the synchronous generator model and the oscillograms and analytical expression of the field current during the short circuit are presented in Section 2. A detailed description and the mathematical formulation of the proposed hybrid metaheuristic algorithm are given in Section 3. Section 4 shows the results of the simulations carried out in this article. Finally, the conclusions are provided in Section 5.

II. SYNCHRONOUS GENERATOR MODEL AND FIELD CURRENT WAVEFORM

A synchronous machine consists of three armature coils, the field coil, and the damper coil, for which the voltage equations can be derived in terms of resistances and self and mutual inductances. Taking into account that coils of the machine are in relative motion, many of the inductances are a function of the position of the rotor. Therefore, the armature variables are transformed into a new variable related to a reference frame fixed to the field system. The mentioned approach is called Park's transformations and is the most widely used for the analysis of synchronous machines. According to this theory, the machine is represented in a two-axis frame consisting of a direct axis (d-axis) and a quadrature axis (q-axis). The direct- and quadrature-axis currents are defined as the currents in two fictitious coils (D and Q) that are located on the corresponding axes, which would set up the same magnetomotive force wave as the actual currents in real armature windings (i_a, i_b, and i_c) [2].

The order of the machine model is directly dependent on the chosen number of damper windings [2]. In this article, a simple model with one damper winding on each axis is considered. According to this, besides the armature windings D and Q, there are three more windings in the machine: the field winding (F), the damper winding on the direct axis (KD), and the damper winding on the quadrature axis (KQ). The described two-axis machine model used in this article is graphically represented in Fig. 1.

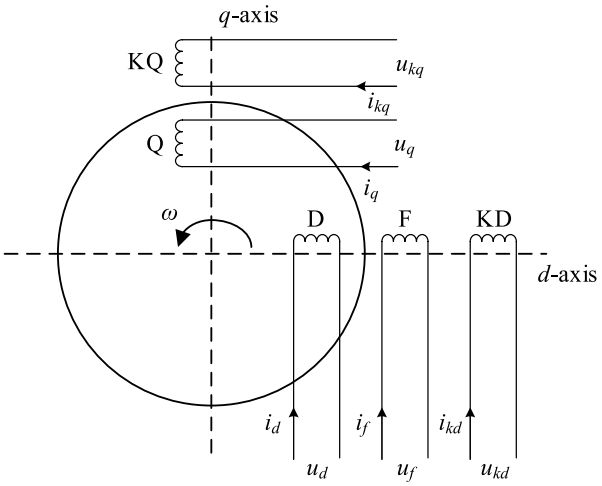

FIGURE 1. Two-axis model of the synchronous machine.

The basis of the two-axis theory is set up by writing the voltage equations for each winding (1)–(5):

$$u_d = R_a i_d + \frac{d\psi_d}{dt} + \omega\psi_q \tag{1}$$

$$u_q = R_a i_q + \frac{d\psi_q}{dt} - \omega\psi_d \tag{2}$$

$$u_f = R_f i_f + \frac{d\psi_f}{dt} \tag{3}$$

$$u_{kd} = R_{kd} i_{kd} + \frac{d\psi_{kd}}{dt} = 0 \tag{4}$$

$$u_{kq} = R_{kq} i_{kq} + \frac{d\psi_{kq}}{dt} = 0 \tag{5}$$

where u, i, R, ω, and ψ are the voltage, current, resistance, angular speed, and flux linkage, respectively. Subscripts refer to the corresponding windings: d – direct axis winding, a – armature winding, q – quadrature axis winding, f – field winding, kd – d-axis damper winding, and kq – q-axis damper winding. Assuming that L_{md} and L_{mq} indicate the mutual inductances between the windings on the d-axis and q-axis, respectively, the flux linkages of the windings are expressed using the following equations:

$$\psi_d = (L_{md} + L_a)\, i_d + L_{md} i_f + L_{md} i_{kd} \tag{6}$$

$$\psi_q = \left(L_{mq} + L_a\right) i_q + L_{mq} i_{kq} \tag{7}$$

$$\psi_f = \left(L_{md} + L_f\right) i_f + L_{md} i_d + L_{md} i_{kd} \tag{8}$$

$$\psi_{kd} = (L_{md} + L_{kd})\, i_{kd} + L_{md} i_f + L_{md} i_d \tag{9}$$

$$\psi_{kq} = \left(L_{mq} + L_{kq}\right) i_{kq} + L_{mq} i_q \tag{10}$$

where L_a, L_f, L_{kd}, and L_{kq} denote the leakage inductances of the armature, field, d-axis damper, and q-axis damper windings, respectively. The equivalent circuits of the synchronous machine are represented in Figs. 2 and 3, where Fig. 2 corresponds to the d-axis and Fig. 3 corresponds to the q-axis. One can note that in equivalent circuits, inductances (L) are replaced by the corresponding reactances ($X = \omega L$).

The method presented in this article relies on the field current waveform during a sudden short-circuit test of an unloaded generator. The analytical expression for the field current during the short circuit is derived in [2] using the previously described two-axis model and is given by the following equation:

$$i_f(t) = i_{f0} + i_{f0}\left(\frac{X_d - X'_d}{X'_d}\right) \times \left[e^{-\frac{t}{T'_d}} - \left(1 - \frac{T_{kd}}{T''_d}\right) e^{-\frac{t}{T''_d}} - \frac{T_{kd}}{T''_d} e^{-\frac{t}{T_a}} \cos(\omega_0 t)\right] \tag{11}$$

where i_f is the field current, t denotes time, i_{f0} denotes the field current before the short circuit and is considered to be known, and ω_0 is the speed during the short circuit and is assumed to be constant and equal to the synchronous speed. The parameters of the synchronous generator that appear in (11) are the direct-axis synchronous reactance (X_d), direct-axis transient reactance (X'_d), direct-axis transient short-circuit time constant (T'_d), direct-axis damper leakage time constant (T_{kd}), direct-axis subtransient short-circuit time constant (T''_d), and armature winding time constant (T_a). The relation between the parameters from equivalent circuits and the parameters from (11) is represented by the equations given in (12)–(17):

$$X_d = X_{md} + X_a \tag{12}$$

$$X'_d = X_a + \frac{X_{md} X_f}{X_{md} + X_f} \tag{13}$$

$$T'_d = \frac{1}{\omega_0 R_f}\left(X_f + \frac{X_{md} X_a}{X_{md} + X_a}\right) \tag{14}$$

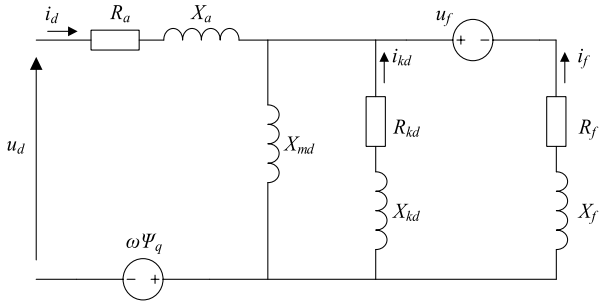

FIGURE 2. Equivalent circuit of d-axis.

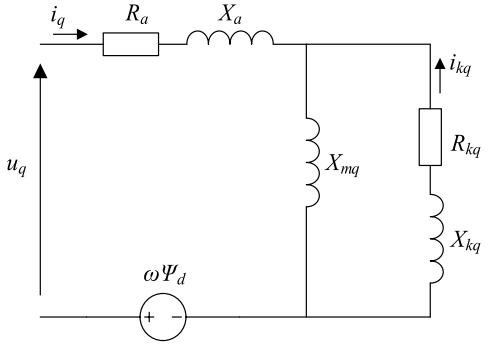

FIGURE 3. Equivalent circuit of q-axis.

$$T_{kd} = \frac{X_{kd}}{\omega_0 R_{kd}} \tag{15}$$

$$T''_d = \frac{1}{\omega_0 R_{kd}} \left(X_{kd} + \frac{X_{md} X_a X_f}{X_{md} X_a + X_{md} X_f + X_a X_f} \right) \tag{16}$$

$$T_a = \frac{X_a}{\omega_0 R_a} \tag{17}$$

In this article, a sudden three-phase short circuit of the generator is carried out in order to obtain an experimental waveform of the field current. This obtained current is compared to the one calculated by the analytical expression given by (11). The parameters defined by (12)–(17) are extracted by using the novel metaheuristic algorithm proposed in this article. The estimated parameters of the generator are calculated so that the objective function, defined as the normalized sum of squared errors (NSSE), is minimized:

$$NSSE\,(\boldsymbol{\theta}) = \frac{\sum_{k=1}^{N} \left(I_{f,exp}\,(k) - I_{f,sim}\,(k) \right)^2}{\sum_{k=1}^{N} I_{f,exp}\,(k)^2} \tag{18}$$

In the previous expression, $I_{f,exp}$ and $I_{f,sim}$ are the experimental and simulated field currents and N is the number of measurements. The vector of estimated parameters is denoted as $\boldsymbol{\theta} = \{X_d, X'_d, T'_d, T_{kd}, T''_d, T_a\}$.

III. ADAPTIVE BLACK WIDOW OPTIMIZATION ALGORITHM (ABWO)

This article presents a novel metaheuristic algorithm based on the existing Black Widow Optimization (BWO) algorithm [48]. The proposed modification relies on adaptive change of the parameters of the algorithm, which are assumed to be constant in [48]. This approach provides an increase in the convergence speed as well as in the accuracy of the results.

The proposed algorithm, like any other metaheuristic algorithm, starts with a randomly initialized population. The population consists of black widow spiders, each of which represents a potential solution to the optimization problem. For the d-dimensional optimization problem, each spider is an array of d elements, called optimization variables (x_1–x_d):

$$\boldsymbol{spider} = \begin{bmatrix} x_1 & x_2 & \ldots & x_d \end{bmatrix} \tag{19}$$

Therefore, the population of black widow spiders is a matrix of size $N \times d$, where N stands for the size of the population (number of spiders). After initialization, the second step of the algorithm is the mating process, which is also called procreation or crossover. It is necessary to randomly choose two parents from the population, denoted as $\boldsymbol{x}_1$ and $\boldsymbol{x}_2$, which are used to create the $\boldsymbol{y}$ offspring ($\boldsymbol{y}_1$ and $\boldsymbol{y}_2$) using (20):

$$y = \begin{cases} \boldsymbol{y}_1 = \boldsymbol{\alpha}\,(\boldsymbol{x}_1) + (1 - \boldsymbol{\alpha})\,\boldsymbol{x}_2 \\ \boldsymbol{y}_2 = \boldsymbol{\alpha}\,(\boldsymbol{x}_2) + (1 - \boldsymbol{\alpha})\,\boldsymbol{x}_1 \end{cases} \tag{20}$$

where $\boldsymbol{\alpha}$ stands for the vector of random numbers in the range from 0 to 1, whose size is $1 \times d$. The number of spiders from the population that take part in the process of mating is defined by the procreation rate (PR).

The third step of the algorithm is related to the cannibalistic behavior that is often exhibited in invertebrates like spiders, scorpions, and so on. Two types of cannibalism are observed in the behavior of the spiders:

- The first is sexual cannibalism, in which the female spider eats the male during or after the mating process. In the optimization algorithm, male and female are identified according to the fitness function value.
- The second type of cannibalism is sibling cannibalism, in which the strong spiderlings eat their weaker siblings. The cannibalism rate (CR) defines the number of siblings that will be eaten during the cannibalism process.

The final stage of the BWO algorithm is the mutation process. The number of spiders from the population that will be mutated is determined by the mutation rate (MR). Namely, during the mutation, each of the selected spiders randomly exchanges two elements (optimization variables) in the array, as graphically represented in Fig. 4.

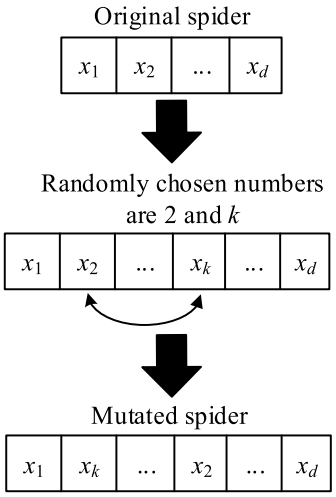

FIGURE 4. Graphical illustration of the mutation process.

The described phases are iteratively repeated until the stopping criterion is reached. Among the final population, the spider with the lowest fitness function value represents the globally optimal solution to the optimization problem. The parameters that are essential for exploring the global search space and escaping from local optima are the procreation rate, cannibalism rate, and mutation rate. Properly chosen values of the mentioned parameters control the balance between exploration and exploitation. The procreation rate defines the production of different offspring, thereby providing diversification and exploration of the search space. Unlike the procreation rate, the mutation rate ensures high performance in the exploitation stage. In [48], these parameters are assumed to be constant: $PR = 0.6$ and $MR = 0.4$. This article presents the adaptive approach embedded in the BWO algorithm, obtaining a novel adaptive BWO (ABWO)

TABLE 1. Pseudo-code of the ABWO Algorithm.

Pseudo-code of ABWO Algorithm
Input data: max_ite, CR, PR_{min}, PR_{max}, MR_{min}, and MR_{max}
Initialize the random population of spiders
Set $ite = 1$
While ($ite \leq max\_ite$)
Calculate the procreation and mutation rates using (21) and (22)
Based on the value of the procreation rate, calculate the number of spiders that will take part in reproduction "nr"
Select the "nr" best solutions from the population and save them in a temporary population called $pop1$
For $i = 1{:}nr$
Randomly select two solutions as parents from $pop1$
Generate the children using (20) (procreation)
Destroy the father (sexual cannibalism)
Destroy a certain number of children spiders according to the value of the cannibalism rate (sibling cannibalism)
Save the remaining solutions in another temporary population $pop2$
End For
Compute the number of mutated spiders "nm" according to the mutation rate
For $i = 1{:}nm$
Select the solution from $pop1$
Generate a new solution by mutating the previously selected one, as described in Fig. 4
Save the new solution in a temporary population $pop3$
End For
Update the population by merging $pop2$ and $pop3$: $population = pop2 + pop3$
Compute the fitness of each spider and update the best solution
$ite = ite + 1$
End While
Return the optimal global solution

algorithm. Namely, in early iterations, global exploration of the search space is much more important than exploitation in order to avoid local optimum solutions. Furthermore, in late iterations, since the global search of the space has already been performed, it is necessary to perform exploitation (local search) of the optimum solutions obtained. Taking these facts into account, it is obvious that the procreation rate, which ensures the exploration, is supposed to have a higher value during early iterations of the algorithm and a lower value in later ones. Similarly, the mutation rate, whose role is to force the exploitation phase, should increase its value as the iterations proceed. Therefore, in this article, an adaptive change of the parameters PR and MR is proposed, according to the following equations:

$$PR = PR_{max} - (PR_{max} - PR_{min}) \frac{ite}{max\_ite} \tag{21}$$

$$MR = MR_{min} + (MR_{max} - MR_{min}) \frac{ite}{max\_ite} \tag{22}$$

where PR_{min}, PR_{max}, MR_{min}, and MR_{max} stand for the minimum and maximum values of the procreation rate and mutation rate, respectively, ite is the current iteration, and max_ite denotes the maximum number of iterations.

The pseudo-code of the proposed algorithm is summarized in Table 1, while the steps of the algorithm are graphically depicted in the flowchart given in Fig. 5.

Finally, the computational efficiency of the proposed ABWO algorithm can be demonstrated by calculating its computational complexity. The Big-O notation is the most common way used to depict computational complexity. According to this, the computational complexity of the ABWO algorithm is denoted as O(ABWO) and it consists of the following components:

1) Problem definition: $O(1)$.
2) Initialization: $O(N \times d)$.
3) Function evaluations: $O(max\_ite \times N \times c)$.
4) Calculating MR and PR: $O(2 \times max\_ite)$.
5) Updating the population: $O(max\_ite \times N \times d)$.

where c stands for the cost of fitness function evaluation. Therefore, the total computational complexity can be calculated using the following equation:

$$\begin{aligned} O\,(\text{ABWO}) &= O\,(1) + O\,(N \times d) + O\,(max\_ite \times N \times c) \\ &\quad + O\,(2 \times max\_ite) + O\,(max\_ite \times N \times d) \\ &= O\begin{pmatrix} 1 + N \times d + max\_ite \times N \times c \\ +2 \times max\_ite + max\_ite \times N \times d \end{pmatrix} \end{aligned} \tag{23}$$

IV. SIMULATION RESULTS

In order to demonstrate the improvement made by the proposed algorithm, in this section, the parameters of the generator are estimated by applying both the original BWO algorithm and the proposed ABWO algorithm. The parameters estimation procedure is based on measuring the field current during the sudden three-phase short-circuit test, as described in Section 2.

After that, the capability of the proposed algorithm to deal with high-dimensional problems and handle the problem of premature convergence is discussed. The experiment is carried out on a synchronous generator in the Bajina Basta hydropower plant, whose basic data are 15.65 kV, 100 MVA, and $\cos\varphi = 0.95$. To conduct a fair comparison, the simulations were performed using the same personal computer, with the following hardware settings: AMD A4 CPU 4 × 2.5 GHz, 4 GB RAM, and 1 TB hard drive. Also, the simulations are carried out in Matlab R2019b, on the operating system

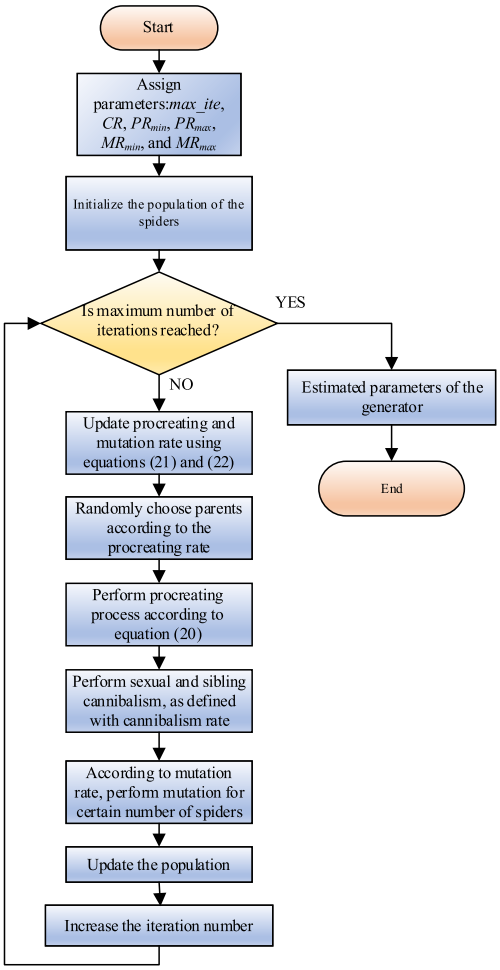

FIGURE 5. Flowchart of the proposed ABWO algorithm.

Windows 10. The objective function, which is minimized in the BWO and ABWO algorithms, is given in (18).

Furthermore, the parameters of the BWO and ABWO algorithms are as follows: the population size is 30, the maximum number of iterations is 40, $CR = 0.5$, $PR_{min} = 0.6$, $PR_{max} = 0.8$, $MR_{min} = 0.2$, and $MR_{max} = 0.4$. Finally, the upper and lower bounds of each optimization variable (parameters of the generator) are defined in Table 2.

TABLE 2. Bounds of the optimization variables.

Parameter	Lower Bound	Upper Bound
X_d (Ω)	2	2.5
X_d' (Ω)	0.7	0.8
T_d' (s)	2	2.5
T_{kd} (s)	0.02	0.04
T_d'' (s)	0.04	0.05
T_a (s)	0.2	0.3

It is very important to highlight that the terminal voltage of the generator during the short-circuit ytest must be reduced in order to protect the armature winding. In the experiment presented in this article, the terminal voltage before the short-circuit test is set as 20% of the nominal one. The results obtained by the proposed method are compared with the parameters measured using standard IEEE tests [4], the parameters from the catalog data provided by VA Tech, and the parameters obtained by the method presented in [41]. The values of the parameters are presented in Table 3, along with the values of the NSSE for each method.

By observing the results presented in the previous table, it can be noted that the best match with the experimental results, measured by the value of the NSSE, is provided by the parameters estimated by the proposed ABWO algorithm. Additionally, Fig. 6 presents a graphical comparison of the field current waveform obtained by the experimental measurement with the field current determined using the analytical expression applying parameters calculated by the ABWO algorithm, by the numerical-based algorithm presented in [41], and by IEEE standard test procedures.

In order to additionally demonstrate the accuracy of the results obtained by the ABWO algorithm, a short-circuit test of the generator was carried out at the moment when the terminal voltage was at 30% and 50% of the nominal value.

A graphical presentation of the experimental and analytical field current waveforms with the parameters calculated using different methods is given in Fig. 7 (for a terminal voltage whose value is 30% of the nominal value). The same comparison, but with voltage before the short circuit set to 50% of the nominal value, is presented in Fig. 8.

Based on these figures, it can be concluded that, in all considered cases, the application of the ABWO algorithm ensures the best match with the experimental results. Therefore, the proposed algorithm outperforms other considered methods used for the determination of the synchronous machine parameters.

Furthermore, a detailed comparative analysis between the proposed ABWO algorithm and the original BWO algorithm, Henry gas solubility optimization (HGSO) algorithm [49], grey wolf optimizer (GWO) algorithm [50], and harris hawks optimization (HHO) algorithm [51], [52] is carried out.

As highlighted in Section 3, the adaptive approach proposed in this article is supposed to accelerate the convergence of the algorithm. To prove this, Fig. 9 demonstrates the convergence curves of all mentioned algorithms applied to the described problem of estimation of synchronous machine parameters. In order to adequately carry out the statistical analysis, all algorithms have been run independently 10 times. Also, the objective function, the maximum number of iterations, and the population size are the same for all algorithms. It is imperative to highlight that the metaheuristic algorithms have a stochastic nature, so they had to be run independently 10 times or more. The best, worst, mean, and median fitness function values, along with the standard deviation, are presented in Table 4. The presented results show that the least values of best, worst, mean, median, and standard deviation results are obtained

TABLE 3. Values of the parameters determined by different methods.

Parameter	ABWO	BWO	[41]	IEEE tests	VA Tech
X_d (Ω)	2.1518	2.1586	NR*	2.1474	2.1005
X_d' (Ω)	0.7652	0.7668	0.7489	0.7441	0.7597
T_d' (s)	2.1990	2.1821	2.0650	2.3100	2.0730
T_{kd} (s)	0.0315	0.0310	0.0330	0.0300	NR**
T_d'' (s)	0.0422	0.0419	0.0410	0.0466	0.0457
T_a (s)	0.2279	0.2302	0.2480	0.2630	NR**
NSSE	4.86×10^{-4}	4.87×10^{-4}	14.25×10^{-4}	13.76×10^{-4}	14.92×10^{-4}

* NR denotes not reported as in [41], the parameter X_d was not estimated by the algorithm proposed in that paper but was measured using the standard IEEE test.
** The VA Tech catalog did not provide information about the values of the parameters T_{kd} and T_a. In order to carry out the comparison, the values obtained with IEEE tests were adopted.

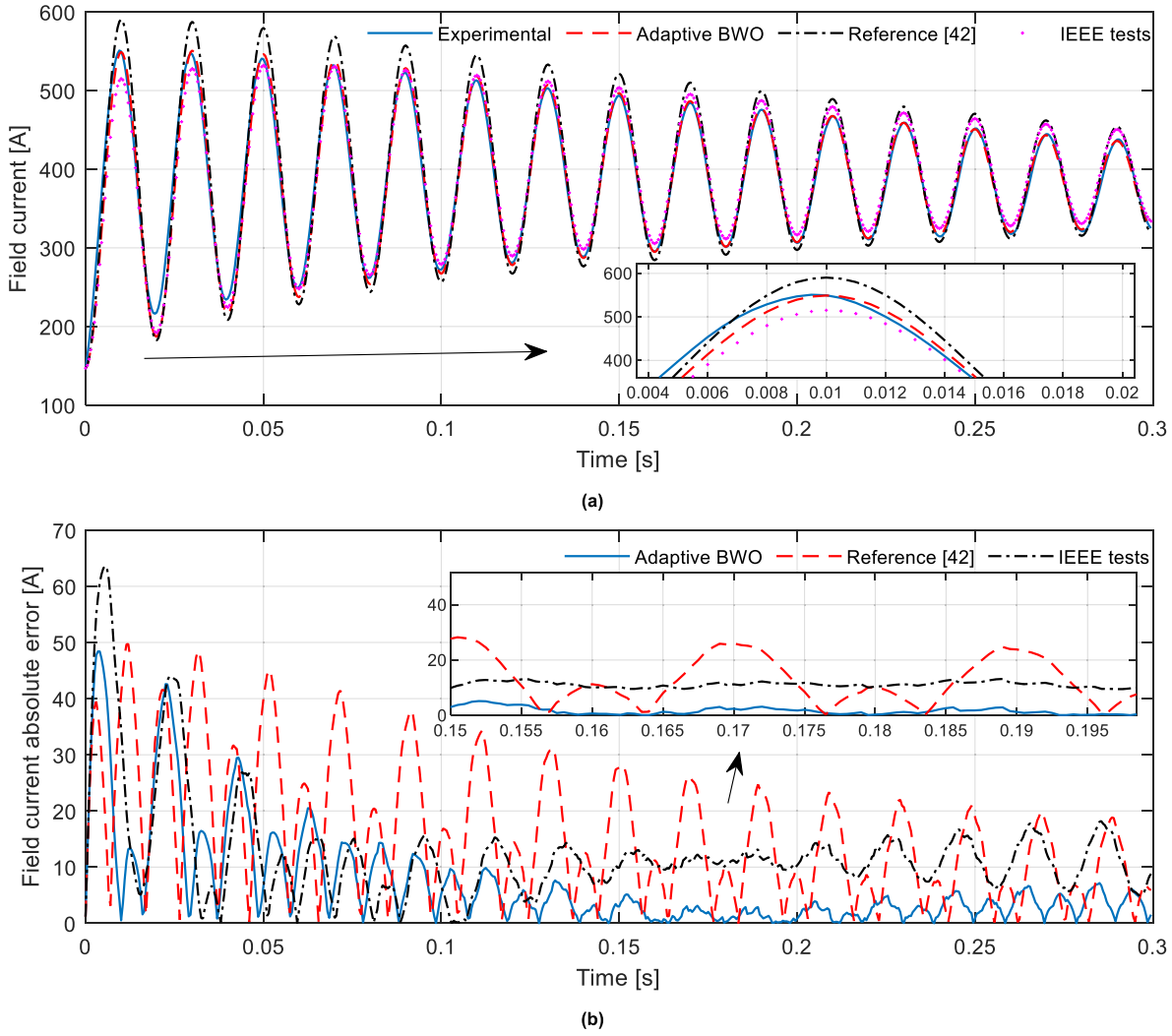

FIGURE 6. Comparison of results obtained: (a) Graphical comparison of experimental and analytical field current waveforms (at 20% of nominal voltage); (b) absolute error between simulation and experimental results.

with the proposed ABWO algorithm, which clearly demonstrates its superiority over other algorithms considered for comparison.

As shown in Table 4, the standard deviation has the lowest value when the proposed ABWO algorithm is applied, which means that the deviation of the results obtained by

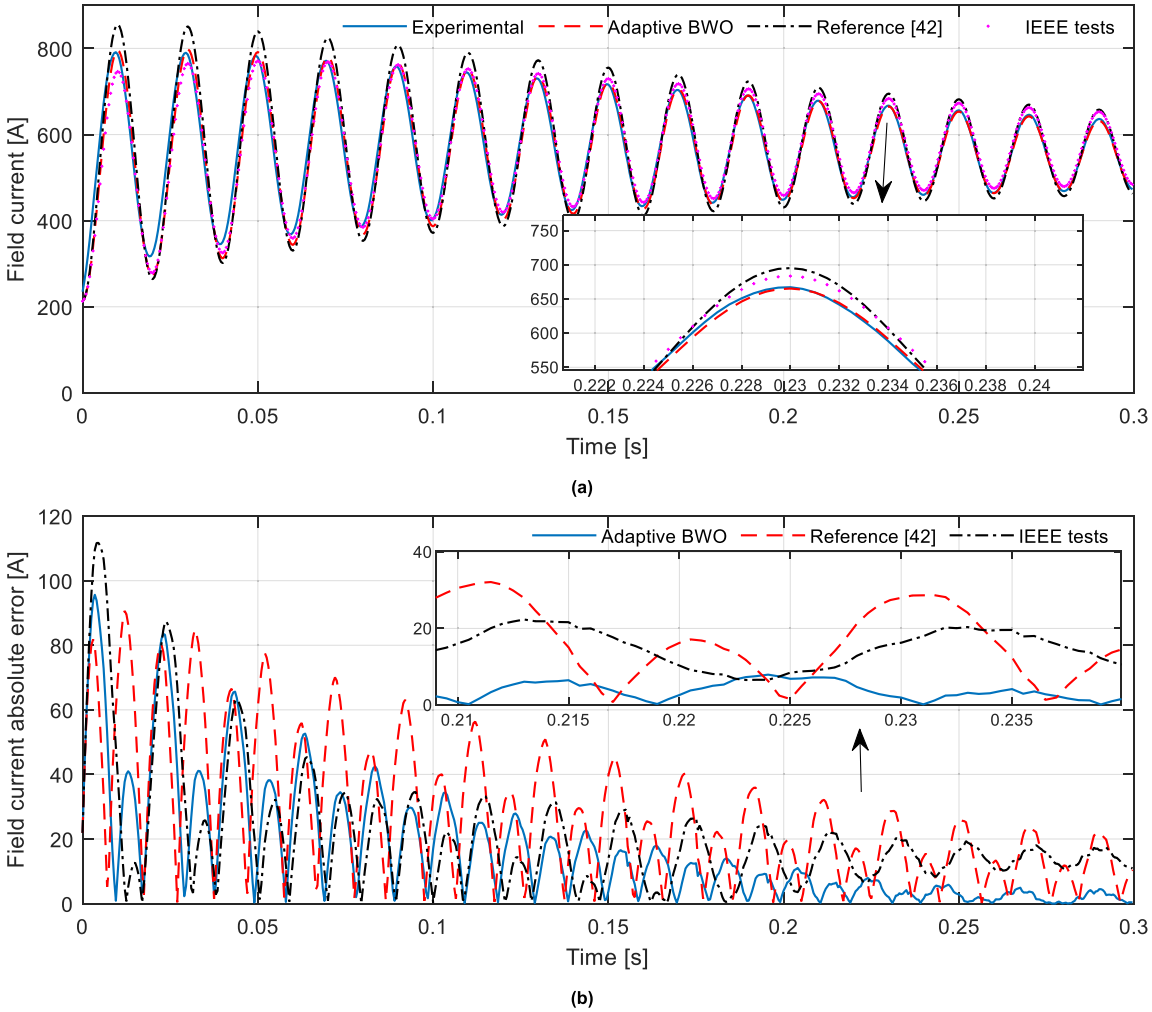

FIGURE 7. Comparison of results obtained: (a) Graphical comparison of experimental and analytical field current waveforms (at 30% of nominal voltage); (b) absolute error between simulation and experimental results.

TABLE 4. Comparison of results obtained with different algorithms.

Algorithm	Best	Worst	Mean	Median	Standard deviation
ABWO	4.86×10^{-4}	4.98×10^{-4}	4.92×10^{-4}	4.90×10^{-4}	3.83×10^{-6}
BWO	4.87×10^{-4}	5.14×10^{-4}	4.95×10^{-4}	4.92×10^{-4}	8.40×10^{-6}
GWO	4.89×10^{-4}	5.26×10^{-4}	5.06×10^{-4}	5.08×10^{-4}	1.23×10^{-5}
HHO	4.86×10^{-4}	5.38×10^{-4}	5×10^{-4}	4.95×10^{-4}	1.53×10^{-5}
HGSO	5.21×10^{-4}	6.12×10^{-4}	5.59×10^{-4}	5.57×10^{-4}	2.89×10^{-5}

TABLE 5. p-values obtained with Wilcoxon's rank-sum test (5% level of significance between the ABWO and other optimization methods).

Algorithms	ABWO vs. BWO	ABWO vs. GWO	ABWO vs. HHO	ABWO vs. HGSO
p-value	3.02×10^{-10}	1.89×10^{-16}	3.65×10^{-14}	8.09×10^{-17}

each run is extremely small. In other words, the results obtained from every run are consistent. Due to the stochastic nature of these types of algorithms, the results obtained from every independent run are not precisely the same. Therefore, the results obtained as the final solution are the ones that provide the minimum fitness function value of all runs. The synchronous generator parameters presented in Table 3 provided the minimum fitness function value (4.86×10^{-4}) from all the independent runs.

Additionally, a non-parametric statistical test called Wilcoxon's rank-sum test is carried out to compare the proposed ABWO algorithm and BWO, GWO, HHO, and HGSO algorithms. The corresponding p-values obtained by applying this test are presented in Table 5, with the 5% level of significance between the ABWO and other optimization methods. The results shown in Table 4 and Table 5 validate the superiority of the ABWO algorithm over the other considered algorithms [53].

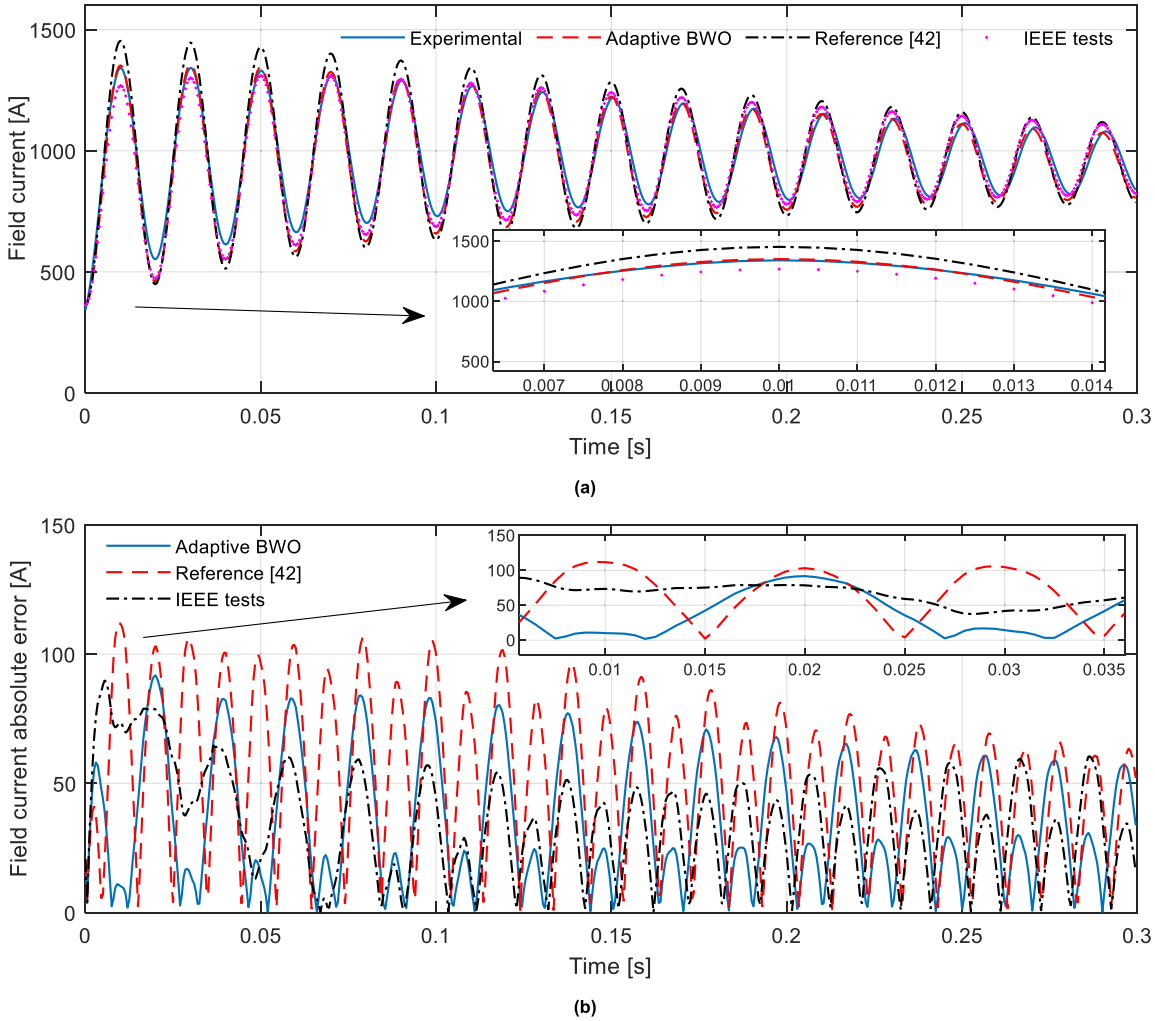

FIGURE 8. Comparison of results obtained: (a) Graphical comparison of experimental and analytical field current waveforms (at 50% of nominal voltage); (b) absolute error between simulation and experimental results.

TABLE 6. Results of ABWO algorithm for different benchmark functions.

Function	Global optimum	ABWO algorithm		
		Best	Mean	Median
$F1=\sum_{i=1}^{d} x_i^2$	0	2.62×10^{-12}	4.83×10^{-12}	5.04×10^{-12}
$F2=\sum_{i=1}^{d}\left(x_i^2-10\cos(2\pi x_i)+10\right)$	0	3.18×10^{-12}	8.16×10^{-12}	8.41×10^{-12}
$F3=-20\exp\left(-0.2\sqrt{\frac{1}{d}\sum_{i=1}^{d} x_i^2}\right)-\exp\left(\frac{1}{d}\sum_{i=1}^{d}\cos(2\pi x_i)\right)+20+e$	0	7.99×10^{-15}	1.79×10^{-4}	1.53×10^{-2}
$F4=\sum_{i=1}^{d}\frac{x_i^2}{4000}-\prod_{i=1}^{d}\cos\left(\frac{x_i}{\sqrt{i}}\right)+1$	0	2.39×10^{-14}	2.35×10^{-2}	1.53×10^{-2}
$F5=\sum_{i=1}^{d} x_i^6\left(2+\sin\frac{1}{x_i}\right)$	0	3.38×10^{-56}	7.42×10^{-21}	1.01×10^{-32}

The scalability of metaheuristic algorithms and their ability to escape from local solutions are significant characteristics of the optimization algorithms. The scalability of an algorithm stands for its ability to deal with high-dimensional problems. The scalability of the algorithm presented in this article is proven by applying it to two well-known benchmark

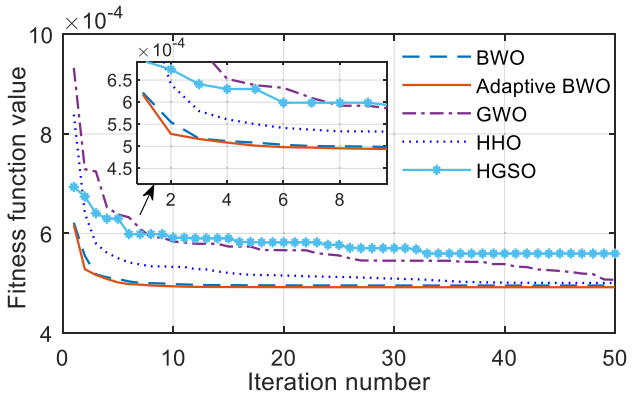

FIGURE 9. Comparison of the convergence curves of ABWO and other algorithms.

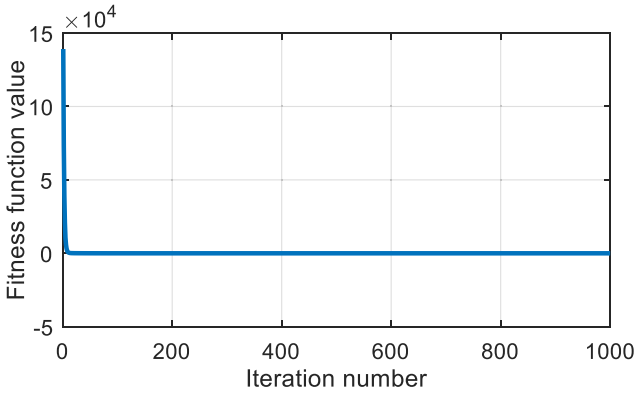

FIGURE 10. Convergence curve of the ABWO algorithm for benchmark function F1.

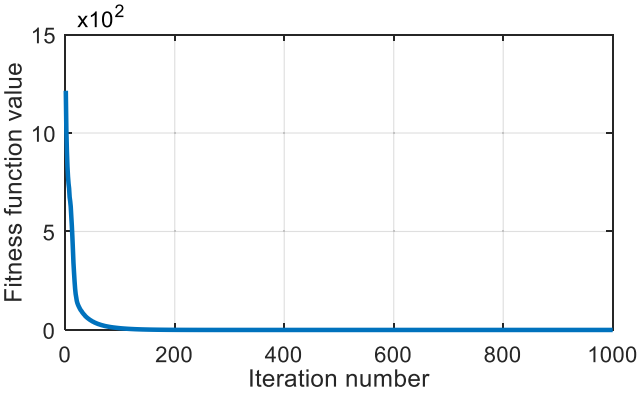

FIGURE 11. Convergence curve of the ABWO algorithm for benchmark function F2.

functions used in [48]. The first one is the sphere function, denoted as F1, and the second is the Rastrigin function, which is denoted as F2. Their mathematical formulation, real global optimal solution, and the optimal solution obtained by the ABWO algorithm are depicted in Table 6. The convergence curves of the ABWO algorithm used for these test functions are presented in Fig. 10 (for F1) and Fig. 11 (for F2). Number of independent runs is set to be 10, the dimension of the problem is $d = 100$, population size $N = 500$, and the maximum number of iterations max_ite=1000.

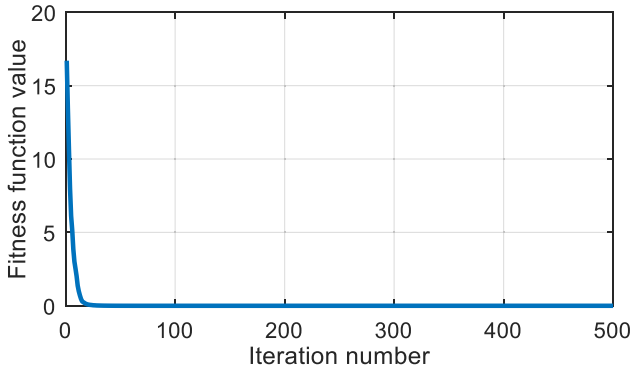

FIGURE 12. Convergence curve of the ABWO algorithm for benchmark function F3.

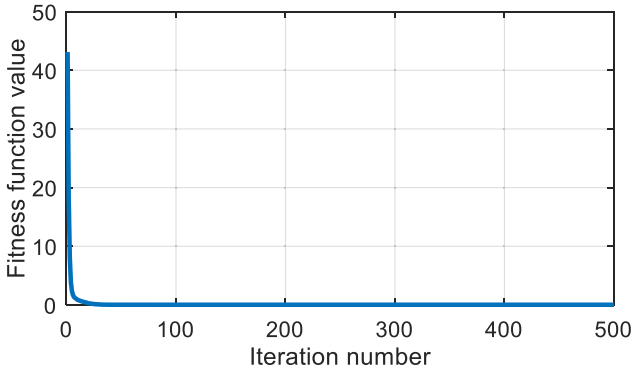

FIGURE 13. Convergence curve of the ABWO algorithm for benchmark function F4.

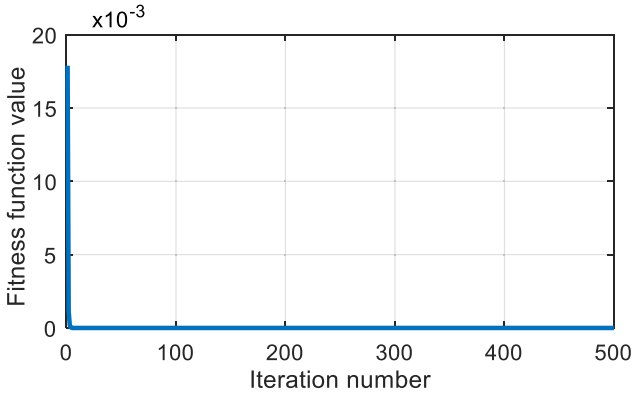

FIGURE 14. Convergence curve of the ABWO algorithm for benchmark function F5.

Moreover, the proposed algorithm's ability to avoid premature convergence, i.e., to escape from local solutions, is discussed. In [48], a certain number of multimodal benchmark functions are used to prove the ability to avoid premature convergence. Many local optimal solutions characterize multimodal functions. According to this, three of the popular multimodal benchmark functions were applied in this article to prove the proposed algorithm's ability to escape from local optimal solutions. Selected benchmark functions are Ackley function (marked as F3), Griewank function (marked as F4), and Csendes function (marked as F5). Like the previously mentioned benchmark functions, Table 6 presents

mathematical formulations of these functions, their optimal global solutions, and the solution obtained by the proposed ABWO algorithm. When applying benchmark functions F3, F4, and F5, dimension size is set to be $d = 10$, population size $N = 100$, the maximum number of iterations *max_ite*=500, and the number of independent runs is 10. Figures 12, 13, and 14 depict the convergence curves of the ABWO algorithm for benchmark functions F3, F4, and F5, respectively.

Based on the presented results, it can be concluded that the proposed ABWO algorithm almost reaches the exact global optimal solution for high-dimensional problems, which validates that the ABWO algorithm can be used to solve the problem of synchronous generator parameters estimation efficiently, as well as other high-dimensional optimization problems. Moreover, the ABWO algorithm was successfully applied for solving benchmark functions F3, F4, and F5, which proves that the ABWO algorithm can easily handle the problem of premature convergence.

V. CONCLUSION

This article proposes a novel method for the estimation of synchronous machine parameters. The first step of the proposed method is measuring the field current during the short-circuit test, while the second step consists of extracting the generator parameters from the obtained field current waveform using the novel algorithm proposed in this article, called the adaptive black widow optimization (ABWO) algorithm. The validation is carried out by comparing the simulation results when the parameters are determined by various methods with experimentally obtained results. Furthermore, a short-circuit experiment test is carried out when the terminal voltage of the generator is 20, 30, and 50% of the nominal value. The proposed method is proven to outperform other considered methods that are used for determination of the machine parameters. Also, this article presents a comparison between the proposed ABWO algorithm and BWO, GWO, HHO, and HGSO algorithms.

By observing the convergence curves, as well as statistical parameters such as the best, worst, mean, median, and standard deviation of the fitness function values, it can be concluded that the ABWO algorithm outperforms the other algorithms considered for comparison. Finally, it is important to point out that the optimization problem solved in this work could be solved by different computational intelligence algorithms as MBO, EWA, EHA, MSA, and others.

ACKNOWLEDGMENT

The authors would like to thank Bajina Basta hydropower plant, Serbia, for the experimental results provided in this work.

REFERENCES

[1] T. A. Lipo, *Analysis of Synchronous Machines*, 2nd ed. Boca Raton, FL, USA: CRC Press, 2017.

[2] B. Adkins and R. G. Harley, *The General Theory Of Alternating Current Machines: Applications to Practical Problems*. Cham, Switzerland: Springer, 1975.

[3] *Rotating Electrical Machines-Part 4: Methods for Determining Synchronous Machine Quantities from Tests*, document IEC 34-4 1985, 1985.

[4] *IEEE Guide: Test Procedures for Synchronous Machines*, Standard 115-1995, 1995.

[5] E. da Costa Bortoni and J. A. Jardini, "Identification of synchronous machine parameters using load rejection test data," *IEEE Trans. Energy Convers.*, vol. 17, no. 2, pp. 242–247, Jun. 2002, doi: 10.1109/TEC.2002.1009475.

[6] R. Wamkeue, F. Baetscher, and I. Kamwa, "Hybrid-state-model-based time-domain identification of synchronous machine parameters from saturated load rejection test records," *IEEE Trans. Energy Convers.*, vol. 23, no. 1, pp. 68–77, Mar. 2008.

[7] R. Wamkeue, C. Jolette, A. B. M. Mabwe, and I. Kamwa, "Cross-identification of synchronous generator parameters from RTDR test time-domain analytical responses," *IEEE Trans. Energy Convers.*, vol. 26, no. 3, pp. 776–786, Sep. 2011, doi: 10.1109/TEC.2011.2140320.

[8] B. Zaker, G. B. Gharehpetian, and M. Karrari, "Improving synchronous generator parameters estimation using $d-q$ axes tests and considering saturation effect," *IEEE Trans. Ind. Informat.*, vol. 14, no. 5, pp. 1898–1908, May 2018, doi: 10.1109/TII.2017.2759502.

[9] G. Gutiérrez Rodríguez, A. Silveira E Silva, and N. Zeni, "Identification of synchronous machine parameters from field flashing and load rejection tests with field voltage variations," *Electr. Power Syst. Res.*, vol. 143, pp. 813–824, Feb. 2017, doi: 10.1016/j.epsr.2016.08.025.

[10] M. A. González-Cagigal, J. A. Rosendo-Macías, and A. Gómez-Expósito, "Parameter estimation of fully regulated synchronous generators using unscented Kalman filters," *Electr. Power Syst. Res.*, vol. 168, pp. 210–217, Mar. 2019, doi: 10.1016/j.epsr.2018.11.018.

[11] J. Huang, K. A. Corzine, and M. Belkhayat, "Online synchronous machine parameter extraction from small-signal injection techniques," *IEEE Trans. Energy Convers.*, vol. 24, no. 1, pp. 43–51, Mar. 2009, doi: 10.1109/TEC.2008.2008953.

[12] A. Rouhani and A. Abur, "Constrained iterated unscented Kalman filter for dynamic state and parameter estimation," *IEEE Trans. Power Syst.*, vol. 33, no. 3, pp. 2404–2414, May 2018, doi: 10.1109/TPWRS.2017.2764005.

[13] B. Ahmadzadeh-Shooshtari, R. Torkzadeh, M. Kordi, H. Marzooghi, and F. Eghtedarnia, "SG parameters estimation based on synchrophasor data," *IET Gener., Transmiss. Distrib.*, vol. 12, no. 12, pp. 2958–2967, Jul. 2018, doi: 10.1049/iet-gtd.2017.1989.

[14] B. Zaker, G. B. Gharehpetian, M. Karrari, and N. Moaddabi, "Simultaneous parameter identification of synchronous generator and excitation system using online measurements," *IEEE Trans. Smart Grid*, vol. 7, no. 3, pp. 1230–1238, May 2016, doi: 10.1109/TSG.2015.2478971.

[15] Y. Xu, L. Mili, M. Korkali, and X. Chen, "An adaptive Bayesian parameter estimation of a synchronous generator under gross errors," *IEEE Trans. Ind. Informat.*, vol. 16, no. 8, pp. 5088–5098, Aug. 2020, doi: 10.1109/TII.2019.2950238.

[16] V. Zimmer, I. C. Decker, and A. S. e Silva, "A robust approach for the identification of synchronous machine parameters and dynamic states based on PMU data," *Electr. Power Syst. Res.*, vol. 165, pp. 167–178, Dec. 2018, doi: 10.1016/j.epsr.2018.09.008.

[17] E. Ghahremani, M. Karrari, and O. P. Malik, "Synchronous generator third-order model parameter estimation using online experimental data," *IET Gener., Transmiss. Distrib.*, vol. 2, no. 5, pp. 708–719, Sep. 2008, doi: 10.1049/iet-gtd:20080175.

[18] A. M. A. Oteafy, J. N. Chiasson, and S. Ahmed-Zaid, "Development and application of a standstill parameter identification technique for the synchronous generator," *Int. J. Electr. Power Energy Syst.*, vol. 81, pp. 222–231, Oct. 2016, doi: 10.1016/j.ijepes.2016.02.030.

[19] E. Kyriakides, G. T. Heydt, and V. Vittal, "On-line estimation of synchronous generator parameters using a damper current observer and a graphic user interface," *IEEE Trans. Energy Convers.*, vol. 19, no. 3, pp. 499–507, Sep. 2004, doi: 10.1109/TEC.2004.832057.

[20] E. Kyriakides and G. T. Heydt, "Estimation of synchronous generator parameters using an observer for damper currents and a graphical user interface," *Electr. Power Syst. Res.*, vol. 69, no. 1, pp. 7–16, Apr. 2004, doi: 10.1016/j.epsr.2003.07.004.

[21] E. Kyriakides, G. T. Heydt, and V. Vittal, "Online parameter estimation of round rotor synchronous generators including magnetic saturation," *IEEE Trans. Energy Convers.*, vol. 20, no. 3, pp. 529–537, 2005.

[22] H. B. Karayaka, A. Keyhani, G. T. Heydt, B. L. Agrawal, and D. A. Selin, "Synchronous generator model identification and parameter estimation from operating data," *IEEE Trans. Energy Convers.*, vol. 18, no. 1, pp. 121–126, Mar. 2003, doi: 10.1109/TEC.2002.808347.

[23] J. J. R. Melgoza, G. T. Heydt, A. Keyhani, B. L. Agrawal, and D. Selin, "Synchronous machine parameter estimation using the hartley series," *IEEE Trans. Energy Convers.*, vol. 16, no. 1, pp. 49–54, Mar. 2001, doi: 10.1109/60.911403.

[24] G. Valverde, E. Kyriakides, G. T. Heydt, and V. Terzija, "Nonlinear estimation of synchronous machine parameters using operating data," *IEEE Trans. Energy Convers.*, vol. 26, no. 3, pp. 831–839, Sep. 2011, doi: 10.1109/TEC.2011.2141136.

[25] H. J. Vermeulen, J. M. Strauss, and V. Shikoana, "Online estimation of synchronous generator parameters using PRBS perturbations," *IEEE Trans. Power Syst.*, vol. 17, no. 3, pp. 694–700, Aug. 2002, doi: 10.1109/TPWRS.2002.800915.

[26] R. Wamkeue, I. Kamwa, X. Dai-Do, and A. Keyhani, "Iteratively reweighted least squares for maximum likelihood identification of synchronous machine parameters from on-line tests," *IEEE Trans. Energy Convers.*, vol. 14, no. 2, pp. 159–166, Jun. 1999, doi: 10.1109/60.766971.

[27] M. Cisneros-González, C. Hernandez, R. Morales-Caporal, E. Bonilla-Huerta, and M. A. Arjona, "Parameter estimation of a synchronous-generator two-axis model based on the standstill chirp test," *IEEE Trans. Energy Convers.*, vol. 28, no. 1, pp. 44–51, Mar. 2013, doi: 10.1109/TEC.2012.2236433.

[28] M. A. Arjona, M. Cisneros-Gonzalez, and C. Hernandez, "Parameter estimation of a synchronous generator using a sine cardinal perturbation and mixed Stochastic–Deterministic algorithms," *IEEE Trans. Ind. Electron.*, vol. 58, no. 2, pp. 486–493, Feb. 2011, doi: 10.1109/TIE.2010.2047833.

[29] M. A. Arjona, C. Hernandez, M. Cisneros-Gonzalez, and R. Escarela-Perez, "Estimation of synchronous generator parameters using the standstill step-voltage test and a hybrid genetic algorithm," *Int. J. Electr. Power Energy Syst.*, vol. 35, no. 1, pp. 105–111, Feb. 2012, doi: 10.1016/j.ijepes.2011.10.003.

[30] M. Dehghani, M. Karrari, W. Rosehart, and O. P. Malik, "Synchronous machine model parameters estimation by a time-domain identification method," *Int. J. Electr. Power Energy Syst.*, vol. 32, no. 5, pp. 524–529, Jun. 2010, doi: 10.1016/j.ijepes.2009.07.010.

[31] P. Kou, J. Zhou, C. Wang, H. Xiao, H. Zhang, and C. Li, "Parameters identification of nonlinear state space model of synchronous generator," *Eng. Appl. Artif. Intell.*, vol. 24, no. 7, pp. 1227–1237, Oct. 2011, doi: 10.1016/j.engappai.2011.05.012.

[32] M. Hasni, O. Touhami, R. Ibtiouen, M. Fadel, and S. Caux, "Estimation of synchronous machine parameters by standstill tests," *Math. Comput. Simul.*, vol. 81, no. 2, pp. 277–289, Oct. 2010, doi: 10.1016/j.matcom.2010.05.010.

[33] F. S. Sellschopp and M. A. Arjona L., "A tool for extracting synchronous machines parameters from the DC flux decay test," *Comput. Electr. Eng.*, vol. 31, no. 1, pp. 56–68, Jan. 2005, doi: 10.1016/j.compeleceng.2004.10.001.

[34] V. A. D. Faria, J. V. Bernardes, and E. C. Bortoni, "Parameter estimation of synchronous machines considering field voltage variation during the sudden short-circuit test," *Int. J. Electr. Power Energy Syst.*, vol. 114, Jan. 2020, Art. no. 105421, doi: 10.1016/j.ijepes.2019.105421.

[35] J. Lidenholm and U. Lundin, "Estimation of hydropower generator parameters through field simulations of standard tests," *IEEE Trans. Energy Convers.*, vol. 25, no. 4, pp. 931–939, Dec. 2010, doi: 10.1109/TEC.2010.2064776.

[36] J. P. Martin, C. E. Tindall, and D. J. Morrow, "Synchronous machine parameter determination using the sudden short-circuit axis currents," *IEEE Trans. Energy Convers.*, vol. 14, no. 3, pp. 454–459, Dec. 1999, doi: 10.1109/60.790896.

[37] E. Mouni, S. Tnani, and G. Champenois, "Synchronous generator modelling and parameters estimation using least squares method," *Simul. Model. Pract. Theory*, vol. 16, no. 6, pp. 678–689, Jul. 2008, doi: 10.1016/j.simpat.2008.04.005.

[38] M. Rasouli and C. Lagoa, "A nonlinear term selection method for improving synchronous machine parameters estimation," *Int. J. Electr. Power Energy Syst.*, vol. 85, pp. 77–86, Feb. 2017, doi: 10.1016/j.ijepes.2016.08.004.

[39] G. Hutchison, D. Giaouris, S. Gadoue, K. Harmer, and B. Zahawi, "Non-invasive identification of turbo-generator parameters from actual transient network data," *IET Gener., Transmiss. Distrib.*, vol. 9, no. 11, pp. 1129–1136, Aug. 2015, doi: 10.1049/iet-gtd.2014.0481.

[40] S. Pillutla, A. Keyhani, and I. Kamwa, "Neural network observers for online tracking of synchronous generator parameters," *IEEE Power Eng. Rev.*, vol. 17, no. 12, pp. 55–56, Aug. 1997.

[41] B. Brkovi, D. Petrovi, and R. Vasi, "Determination of synchronous generator parameters using the field current waveform," in *Proc. 18th Int. Symp. Power Electron.*, Novi Sad, Serbia, Oct. 2015, pp. 1–8.

[42] E. L. Geraldi, T. C. C. Fernandes, A. B. Piardi, A. P. Grilo, and R. A. Ramos, "Parameter estimation of a synchronous generator model under unbalanced operating conditions," *Electr. Power Syst. Res.*, vol. 187, Oct. 2020, Art. no. 106487, doi: 10.1016/j.epsr.2020.106487.

[43] Y. Li, J. Li, J. Qi, and L. Chen, "Robust cubature Kalman filter for dynamic state estimation of synchronous machines under unknown measurement noise statistics," *IEEE Access*, vol. 7, pp. 29139–29148, 2019, doi: 10.1109/ACCESS.2019.2900228.

[44] G.-G. Wang, S. Deb, and Z. Cui, "Monarch butterfly optimization," *Neural Comput. Appl.*, vol. 31, no. 7, pp. 1995–2014, Jul. 2019, doi: 10.1007/s00521-015-1923-y.

[45] G.-G. Wang, S. Deb, and L. dos S. Coelho, "Earthworm optimisation algorithm: A bio-inspired metaheuristic algorithm for global optimisation problems," *Int. J. Bio-Inspired Comput.*, vol. 12, no. 1, pp. 1–22, Jan. 2018, doi: 10.1504/IJBIC.2018.093328.

[46] G.-G. Wang, S. Deb, and L. D. S. Coelho, "Elephant herding optimization," in *Proc. 3rd Int. Symp. Comput. Bus. Intell. (ISCBI)*, Dec. 2015, pp. 1–5, doi: 10.1109/ISCBI.2015.8.

[47] G.-G. Wang, "Moth search algorithm: A bio-inspired Metaheuristic algorithm for global optimization problems," *Memetic Comput.*, vol. 10, no. 2, pp. 151–164, Jun. 2018, doi: 10.1007/s12293-016-0212-3.

[48] V. Hayyolalam and A. A. Pourhaji Kazem, "Black widow optimization algorithm: A novel meta-heuristic approach for solving engineering optimization problems," *Eng. Appl. Artif. Intell.*, vol. 87, Jan. 2020, Art. no. 103249, doi: 10.1016/j.engappai.2019.103249.

[49] F. A. Hashim, E. H. Houssein, M. S. Mabrouk, W. Al-Atabany, and S. Mirjalili, "Henry gas solubility optimization: A novel physics-based algorithm," *Future Gener. Comput. Syst.*, vol. 101, pp. 646–667, Dec. 2019, doi: 10.1016/j.future.2019.07.015.

[50] S. Mirjalili, S. M. Mirjalili, and A. Lewis, "Grey wolf optimizer," *Adv. Eng. Softw.*, vol. 69, pp. 46–61, Mar. 2014, doi: 10.1016/j.advengsoft.2013.12.007.

[51] A. A. Heidari, S. Mirjalili, H. Faris, I. Aljarah, M. Mafarja, and H. Chen, "Harris hawks optimization: Algorithm and applications," *Future Gener. Comput. Syst.*, vol. 97, pp. 849–872, Aug. 2019, doi: 10.1016/j.future.2019.02.028.

[52] A. F. Zobaa, S. H. E. A. Aleem, and A. Y. Abdelaziz, *Classical and Recent Aspects of Power System Optimization*, 1st ed. Waltham, MA, USA: Academic Press, 2018, doi: 10.1016/C2016-0-03379-X.

[53] G.-G. Wang, L. Guo, A. H. Gandomi, G.-S. Hao, and H. Wang, "Chaotic krill herd algorithm," *Inf. Sci.*, vol. 274, pp. 17–34, Aug. 2014, doi: 10.1016/j.ins.2014.02.123.

MIHAILO MICEV (Student Member, IEEE) was born in Podgorica, Montenegro, in 1995. He received the B.Sc. degree in power systems and automatic control and the Spec.Sci. degree in automatic control from the Faculty of Electrical Engineering, University of Montenegro, Podgorica, in 2017 and 2018, respectively. He is currently pursuing the M.Sc. degree. He is currently a Teaching Assistant with the University of Montenegro. His research interests include switched reluctance machines, synchronous and induction machines, metaheuristic algorithms, optimization techniques, automatic voltage regulation, power electronics, and excitation systems of synchronous generator. He is a member of the Study Committee A1–Rotating electrical machines of the Montenegrin Committee of the International Council on Large Electric Systems CIGRE CG KO.

MARTIN ĆALASAN (Member, IEEE) was born in Plužine, Montenegro, in 1986. He received the B.Sc., M.Sc., and Ph.D. degrees in electrical engineering from the University of Montenegro, Podgorica, in 2009, 2010, and 2017, respectively. He is currently working as an Assistant Professor with the Department of Power System and Automatics, University of Montenegro. He is the author or a coauthor of many refereed journal (Edition IEEE, IET, Elsevier, and Springer) and conference papers, and has published more than 130 journal and conference papers. His research interests include induction machine, switched reluctance generator, electrical braking, and excitation systems of synchronous generator and solar energy. He is a member of several international and national organizations and associations (Institute of Electrical and Electronics Engineers (IEEE), Conseil International des Grands Réseaux Electriques (CIGRE), and CIGRE CG KO). He is the Chairman of the Study Committee A1–Rotating electrical machines of the Montenegrin Committee of the International Council on Large Electric Systems CIGRE CG KO. He also serves as the Secretary and a Representative for Montenegro in IEEE Chapter Power and Energy (PE-31).

DRAGAN S. PETROVIĆ was born in Kosanica, Pljevlja, Montenegro, in 1942. He received the B.S. and M.S. degrees in electric power engineering from the Faculty of Electrical Engineering, University of Belgrade, Serbia, in 1964 and 1968, respectively, and the Ph.D. degree in electrical engineering from the Faculty of Electrical Engineering and Computing, University of Zagreb, Croatia. His Ph.D. thesis was on testing of synchronous machines. He was a Retired Professor. He taught at the Faculty of Electrical Engineering, University of Belgrade, Serbia, until retirement in 2009. He has served as the President of CIGRE SC A1 Serbia, from 1991 to 2011.

ZIAD M. ALI received the B.Sc. and M.Sc. degrees in electrical engineering from the Faculty of Engineering, Assiut University, Assuit, Egypt, in 1998 and 2003, respectively, and the Ph.D. degree from Kazan State Technical University, Tatarstan, Russia, in 2010. He has worked as a Demonstrator with the Aswan Faculty of Engineering, South Valley University, Aswan, Egypt. He has worked as an Assistant Lecturer with the Aswan Faculty of Engineering. He has worked as Assistant Professor with the Aswan Faculty of Engineering, from 2011 to 2016, a Visitor Researcher with the Power System Laboratory, Kazan State Energy University, Russia, from 2012 to 2013, and a Visitor Researcher with the Power System Laboratory, College of Engineering, University of Padova, Italy, from 2013 to 2014. He is currently working as an Associate Professor with the Electrical Department, College of Engineering at Wadi Addawasir, Prince Sattam Bin Abdulaziz University, Saudi Arabia. His research interests include power system analysis, FACTS, optimization, renewable energy analysis, smart grid, and material science.

NGUYEN VU QUYNH was born in Vietnam, in 1979. He received the B.Sc. and M.Sc. degrees in electrical engineering from the University of Technical Education, Ho Chi Minh City, Vietnam, in 2003 and 2005, respectively, and the Ph.D. degree in electrical engineering from the Southern Taiwan University of Science and Technology, Tainan, Taiwan, in 2013. He is currently the Vice President of Lac Hong University. His research interest includes control technique.

SHADY H. E. ABDEL ALEEM (Member, IEEE) received the B.Sc. degree from the Faculty of Engineering, Helwan University, Egypt, in 2002, and the M.Sc. and Ph.D. degrees from the Faculty of Engineering, Cairo University, Egypt, in 2010 and 2013, respectively, all in electrical power and machines. Since September 2018, he has been an Associate Professor with the 15th of May Higher Institute of Engineering. His research interests include harmonic problems in power systems, power quality, renewable energy, smart grid, energy efficiency, decision making, optimization, green energy, and economics. He is the author or a coauthor of many refereed journal and conference papers, and has published more than 100 journal and conference papers, 15 book chapters, and six edited books with the Institution of Engineering and Technology (IET), Elsevier, Springer, and InTech publishers, in addition to supervising postgraduate students. He was awarded the State Encouragement Award in Engineering Sciences from Egypt in 2017 and the Medal of Scientific Excellence in Engineering Sciences from Egypt in 2020. He is a member of the Institution of Engineering and Technology (IET) and the Egyptian Sub-Committees of IEC. He is an Editor/Associate Editor of the *International Journal of Renewable Energy Technology*, *International Journal of Electrical Engineering and Education*, and *Vehicle Dynamics*.